Asymptotic residual stresses in butt-welded joints under fatigue loading

P. Ferro[1*], F. Berto[1], M.N. James[2, 3]

[1] Department of Management and Engineering, University of Padova
Stradella San Nicola 3, 36100 Vicenza (Italia)
[2] School of Marine Science and Engineering, University of Plymouth
Drake Circus, Plymouth, England
[3] Department of Mechanical Engineering, Nelson Mandela Metropolitan University
Port Elizabeth, South Africa

*Corresponding author: ferro@gest.unipd.it

ABSTRACT
If a weld toe is modelled as a sharp V-notch angle, the stress distribution near the notch tip is singular. Its intensity can then be quantified by means of Notch Stress Intensity Factors (NSIF), which have been proven to be capable of summarizing the high-cycle fatigue strength of welded joints having very different global and local geometries. When a singular residual stress field induced during solidification of the fusion zone near the weld toe, the local load ratio is modified making the fatigue strength sensitive to residual stresses in the high-cycle regime. However, for an accurate estimation of the fatigue performance of welded joints, it is necessary to consider not only the initial residual stress field but also its variation under load, as both of these may play an important role. In this work the effect of fatigue loading on the asymptotic residual stress redistribution near the weld toe of a butt-welded joint is studied by means of numerical simulations. A model is then proposed to estimate the influence of residual stresses on the fatigue strength of welded joints. Experimental results taken from the literature were found in good agreement with those predicted by the proposed model.

Keywords: *welded joints; residual stresses; strain energy density; thermo-mechanical problems; notch stress intensity factor*

1. Introduction

In order to decrease the environmental impact and increase the efficiency of mechanical structures, the structural weight has to be reduced. Structural weight reduction can be accomplished through the use of high strength or light alloys, and by utilizing materials much closer to their limiting capacity. In this context, it is imperative to make improvements in the fatigue design of welded joints, since welding is generally the weakest point of a mechanical structure subjected to cyclic loading. The fatigue strength of a welded joint is governed by the microstructural defects (such as porosity and inclusions), the geometrical stress concentrating features at the weld toe and weld root (e.g. weld profile and undercut) and the metallurgical notches related to the inhomogeneous microstructure and hardness variations induced by different thermal histories in the various weld zones. Furthermore, residual stress fields will play an important role in either reducing or increasing the fatigue strength of welded joints according to the sign of both the residual stresses and the remotely applied stress. More specifically, the influence of residual stresses on the fatigue strength of welded joints strongly depends on whether their distribution near the most likely sites of failure initiation undergoes relaxation as a result of the cyclic loading. Residual stress relaxation/redistribution is mainly due to plastic effects that arise near the weld toe and weld root. Accordingly, the fatigue strength sensitivity to residual stresses occurs mainly in the high-cycle fatigue regime where

their plasticity-induced redistribution can be neglected. It appears that the earliest experimental evidence of a residual stress effect on welded joints derives from work carried out in the period 1939 - 1958 [1-4]. Early work showed a negligible influence of residual stresses on the fatigue limit of as-welded joints compared with stress-relieved joints. Subsequently, detailed investigation [e.g. 5] demonstrated that an increase in fatigue resistance >150% could be obtained with stress-relieved specimens compared with the as-welded joints. Several papers highlight the strong influence of residual stresses on the fatigue limit of most types of joint [6-8] but their effects are not yet well understood and remain a matter of debate. The principal reasons of this lack of clarity can be found both in the difficulty of determining 3D residual stress distributions in welded structures and the in the complex interaction between the residual stress distribution and the applied loads. For this reason, conservative assumptions are generally made in the current fatigue design of welds. For instance, in fatigue design books [9, 10] and codes [11], residual stresses in welded joints are assumed to be of yield strength magnitude. Certain standards such as BS7910:2013 [A] give guidance on the likely values of residual stress in structures subject to post-weld heat treatment (section 7.1.8.3) in an enclosed furnace. The guidance further notes, however, that where local post-weld heat treatment is carried out no general recommendations can be made. Furthermore, the influences of residual stress and mean stress on fatigue strength are algebraically additive and the effects of relaxation or redistribution under load are not taken into account. Under such conditions, fatigue strength of welded joints can be characterized solely by the stress amplitude. This is a result of the assumption of yield strength residual stress levels existing at welded joints and hence the applied stress cycles down from tensile yield during fatigue loading, irrespective of the mean stress (or load ratio, R) in the applied fatigue cycle [12]. BS 7910 also provides some guidance in Annex Q on residual stress profiles in as-welded joints in terms of flaw assessment [A]. The approach in Annex Q has been validated through work contracted to TWI by the UK Health and Safety Executive (HSE) that considered residual stresses in girth welds. That programme included a brief literature review, residual stress measurements for two types of girth welds, numerical modelling of residual stress profiles and discussion of the impact of the new data on the guidance given in BS 7910 [B].

However, the simplifications mentioned above are not universally applicable. In fact, the assumption that tensile residual stresses as high as the yield stress are always present at the critical points is not proven experimentally and the effect of mean stresses in the case of low residual stresses needs to be clarified quantitatively. Since the improvement of fatigue strength by residual stress relaxation through post welding heat treatments is very expensive, it is important to understand welding residual stresses and their effects under various loading conditions.

In recent years, different local approaches have been developed in order to predict the fatigue strength of welded joints depending on the parameters assumed to be important for fatigue behaviour. Assuming a "*worst case hypothesis*", the weld toe and the weld root regions can be modelled as a pointed V-notch of zero notch root radius and, accordingly, the intensity of the singular stress distribution can be quantified by means of NSIF which have been proven to be effective parameters capable of summarizing the high cycle fatigue strength of welded joints having very different global and local geometries [13-14]. The main drawback of the local stress approach based on NSIF is that it does not allow a direct comparison between the fatigue strength of joints having different opening angles. From a practical point of view this means that data derived from fatigue failure at weld root or at the weld toe cannot be directly compared and must be treated separately. However, this limitation is overcome whenever fatigue strength assessments are based on the averaged Strain Energy Density (SED)

evaluated over a circular sector (structural volume) of radius R_C, as comprehensively discussed by Lazzarin and co-workers [14-15]. The local strain energy density is directly linked to the relevant NSIF for modes I and II and to the size of the control radius, R_C, which depends, in turn, on the material microstructure near the welds. Accordingly, different values of R_C would characterize high power density processes (i.e. laser welding (LW) or electron beam welding (EBW)) compared with arc welding processes. Ferro et al. [16] have demonstrated that the residual stress field, resulting from the solidification and cooling of a molten zone in the vicinity of a V-notch tip, is still singular and that the singularity degree, which depends on the V-notch opening angle, will match the elastic [17] or the elastic-plastic [18] value depending on the magnitude of the thermal loads and clamping conditions. However, due to the complex interactions among thermo-mechanical material properties, clamping conditions, joint geometry, thermal loads and phase transformation, the evaluation of residual stresses is extremely difficult and time consuming, especially near singular points such as the weld toe. In particular, the numerical evaluation of local residual stresses therefore requires reliable finite element models that are able to account for the phase transformation effects [19]. A comprehensive analysis of the effects of phase transformations on residual stresses induced by welding processes can be found in reference [20]. In that work, both volume changes and transformation plasticity associated with phase transformations were taken into account. Such effects were found to have a high influence on the residual stress fields, especially when compared with the results obtained from a simplified single-phase material. The asymptotic residual stress field near a sharp V-notch tip was investigated in references [21, 22]. In this work it was found that, depending on the specimen geometry and the size and shape of the heat affected zone (HAZ), phase transformation effects might change the sign of the singular residual stress field with respect to that calculated using a simplified single-phase material.

When the residual NSIF are used to quantify the influence of residual stresses on the fatigue strength of welded joints, the redistribution/relaxation of the asymptotic stress field near the weld toe induced by the fatigue load has to be investigated. In one recent paper [23], a method based on the LSED approach is proposed and applied in the high-cycle regime where the redistribution of residual stresses induced by plastic effects is negligible (the *small scale yielding* hypothesis). The residual asymptotic stress fields are treated as analogous to a "*mean stress*" field which affects the fatigue strength in the high-cycle regime. On the other hand, in the medium and low-cycle fatigue regime, the residual stress redistribution induced by plastic effects is expected to make the fatigue strength less sensitive to pre-existing residual stresses.

The main thrust in the work reported in the present paper is to investigate the effect of fatigue loading on the asymptotic residual stress redistribution near the weld toe of a butt-welded joint through numerical simulation. A model is then proposed to estimate their influence on fatigue strength of welded joints. Experimental results taken from literature were found in good agreement with those predicted by the model. In addition, the paper commences with a short review of some of the published work that has dealt with the effect of fatigue cycling on the amplitude and direction of residual stress fields.

2. Influence of fatigue loading on residual stress

Residual stresses are an unavoidable consequence of almost all manufacturing and fabrication processes and can also arise during service. They will occur under any set of circumstances that leads to differential expansion or contraction between adjacent parts of a body in which the local yield strength is exceeded. Their subsequent influence on structural reliability

depends on their magnitude, sign and extent relative to the controlling length, area or volume of material associated with any particular mode of failure. As noted in reference C the impact of residual stress is therefore wider than just an effect on fatigue life; depending on the structure, their relaxation can lead to distortion during subsequent machining operations and they can affect aspects of structural integrity such as the buckling of welded columns.

Whilst for many years there has been wide acknowledgement of the beneficial and detrimental effects of residual stress on fatigue life of alloys and structures, their assessment has been rendered difficult by such issues as complexity of measurement and analysis, limited near-surface data resulting from the use of techniques like incremental hole drilling or laboratory X-ray, and substantial repeatability issues arising from inter-laboratory and technique differences. Significant progress has come from the development of high intensity synchrotron X-ray and neutron radiation sources, e.g. the European Synchrotron Radiation Facility (ESRF) and the Institut Laue-Langevin (ILL) in Grenoble, France, as well as from automated sample manipulation stages allowing precise 3D measurements of strain in large structural components. Additionally, it is possible on certain beamlines to apply fatigue loading to specimens in-situ whilst making residual strain measurements that can be subsequently converted to stress. It is also worth noting that the issue of determining multiaxial residual stress distributions from limited experimental datasets has also been considered in the literature, e.g. [D].

Despite these improvements in the capability of assessment of residual stress at welded joints, the level of residual stress is highly variable and depends on many factors such as joint design and component thickness (constraint), peak temperature attained at a point during welding, weld process and heat input, and pre-existing stress level in the components (which has an influence at least in the region away from the weld zone – see reference E) as well as any PWHT of the joint. Whilst this makes the development of standardised procedures for dealing with residual stresses at welds very difficult, it has not prevented some researchers from investigating various aspects of the interaction among welds, residual stress and fatigue. A literature search on ScienceDirect indicates that a relatively small number of papers have reported the results of investigations of weld zone residual stress and their influence on fatigue crack growth [F–H] . A more extensive body of work has considered residual stress relaxation under cyclic loading using either numerical modelling [e.g. I-K] or experimental observations [e.g. L-P].

The work on residual stress influence on fatigue is difficult to summarise in general terms as the individual studies tend to focus on specific joint geometries, e.g. the relatively complex K-joint detail [F]. Reference F considered K-joints in S355 steel where measured residual stress values (using neutron diffraction) at the weld toe are of yield strength magnitude, tested with the chord and one brace member in tension and the second brace member in compression. The authors found that details in tension experienced almost zero-tension loading under an applied stress ratio of 0.1, while the details in compression experienced almost zero-compression loading with $R = 10$. Crack growth at the tensile hot spot stress under tension-tension loading was therefore driven by the applied stresses, and crack growth at the compression hot spot was driven by the tensile residual stress. The tensile residual stresses enabled cracks to grow up to at least half the chord wall thickness under applied compressive stresses. This example illustrates some of the complexities inherent in any standardisation of guidance around the treatment of residual stresses in fatigue life prediction for welded joints.

Work by Bussu and Irving [G] on a friction stir welded aircraft alloy, 2024-T351, presented a review of the influence of fusion weld residual stress fields on fatigue crack growth and the

comparative contributions to crack growth arising from residual stress, heat-affected zone (HAZ) microstructures and hardness levels. Their review showed that the residual stress field plays the dominant role and that, for cracks propagating perpendicular to the weld and subjected to weld-induced residual stresses of at least 0.5 yield, crack growth rates were enhanced by a factor of three to seven times those observed in the parent plate. For cracks initiating in the weld HAZ, where compressive residual stresses were present, crack growth rates were correspondingly slower. In cases where cracks propagated parallel to the weld in the weld metal, growth rates were comparable with those observed in the parent plate. Many of studies reported by Bussu and Irving [G] had proposed that the effects of residual stress on crack growth rates could be explained by crack closure arguments. Their own work [G] in friction stir welds supported these general observations that fatigue crack growth rates depend strongly on their orientation and location relative to the weld line and that the role of residual stresses is dominant and can be explained using closure concepts. Bertini [H] in work on fatigue crack growth at welds in C-Mn structural steel in air and seawater environments, also invoked closure arguments to explain his observation in both air and seawater environments of lower crack growth rates in weld specimens than were observed in parent plate.

The relaxation of residual stress under cyclic loading requires loading into the plastic yielding regime and work by Newby, James and Hattingh [P] has shown that fatigue cycling in four point bend of a shot peened 12CrNiMo martensitic steel with a peak stress of 868 MPa, equal to the 0.2% proof strength, and an amplitude of 40 MPa led to a log-linear decay in residual stress value as a function of number of fatigue cycles; a decline of 28% in residual stress at a point 50 μm below the surface being observed after 10,000 load cycles. In that work, synchrotron X-ray diffraction at the ESRF was used to measure residual stresses (experiment MA-326). In other work on four point bend fatigue loading of friction stir butt welds in 5083-H321 aluminium alloy [O] with a 0.2% proof strength of 263 MPa it was observed that the application of fatigue cycles at R = 0.1with a peak tensile stress of 250 MPa led to a progressive increase in the overall tensile magnitude of the residual stresses transverse to the weld line and to more sharply defined tensile peaks. Thus 100 cycles of fatigue loading produced a fourfold increase in tensile residual stress values from +20 MPa to +80 MPa. Residual stress measurements were made using synchrotron X-ray diffraction at the ESRF (experiment ME-197). These observations were attributed to the weld zone softening that occurs in this strain hardening alloy during welding and to the subsequent strain-induced hardening in the weld zone that occurs during the fatigue cycling. This supports the point made earlier in this paper that the fatigue strength of a weld represents a complex interaction between microstructural defects, geometrical stress concentrating features and the metallurgical aspects related to inhomogeneous microstructure and hardness variations across the weld zone.

Hatamleh, Rivero and Swain [M] have reported residual stresses in shot and laser peened plates of friction stir welded 2195 aluminium-lithium alloy obtained via laboratory X-ray diffraction and the destructive contour method after fatigue cycling with R = 0 and a maximum stress of 75% of the proof strength. Their conclusions were that most of the surface residual stress relaxation in the unpeened FSW sample occurred during the first load cycle and that the greatest amount of stress relaxation in the unpeened samples took place in the weld nugget, which was the weakest part of the weld zone. Lee, Chang and Van Do [J] have reported residual stress relaxation results for steel butt welds obtained from 3D thermo-mechanical FE modelling of weld-induced residual stress and subsequent 3D elastic-plastic FE modelling of their relaxation under cyclic loading. The residual stress model was calibrated against experimental strain gauge measurements of residual stress from a bead-on-plate weld and layer removal measurements on a double-sided ‘V’ butt joint. They considered

cyclic loading cases for six values of load amplitude from 30 MPa to 130 MPa and R = 0.1 with the loads applied either perpendicular to, or parallel with, the weld joint. The room temperature 0.2% proof strength of SM400 steel is around 245 MPa, so that the fatigue cycling with the largest load amplitude exceeds this value. Their conclusions were that the magnitude of the stress relaxation depends on loading direction relative to the weld joint as well as the amplitude of the applied stress. In their work the longitudinal residual stresses were of larger magnitude that the transverse ones, and the stress relaxation was greatest in the longitudinal direction. The authors also noted that lower relaxation of residual stresses was observed near the welding stop-start positions due to the lower restraint at those points.

An interesting observation regarding the effect of cyclic loading on residual strains has been reported by Asquith et al [Q] in work on shot-peened 7050-T7451 aluminium alloy subject to four point bend. Specimens were loaded in fatigue to around 10% of the expected life at R = 0.1 and peak stress levels of 200 MPa (N = 200,000 cycles), 220 MPa (N = 178,500 cycles) and 275 MPa (N = 27,126 cycles). Residual strains were measured using synchrotron X-ray diffraction on the ID31 beamline at the ESRF (experiment ME 7478). At the highest level of applied stress of 275 MPa, an average 15% relaxation in residual strain was observed. Of more interest, however, were observations of a significant change in the angle of the principal strain as a function of depth below the specimen surface at all levels of applied fatigue cycling, compared with the as-peened specimen. The angle switched from 0-10º in the near-surface region to 70-90º in deeper regions. This corresponds approximately with the depth at which maximum compressive strain occurs in the shot-peened region. The depth below the surface at which this switching occurs increases with increasing fatigue load from 0.18 mm to 0.25 mm indicating that applied load has an influence on the strain orientation.

Perhaps the key point arising out of this short review of some of the published work, is that although we now have sophisticated 3D measurements techniques available to us, the cost of a typical synchrotron or neutron experiment is rather high. It is therefore unlikely that engineers will be able to perform the large number of repeat experiments necessary to underpin any changes to the manner in which residual stresses are treated in codes and standards. It is therefore necessary to continue to develop numerical and analytical tools capable of predicting the residual stress profiles at welds, and their influence on, and modification by, fatigue loading. The remainder of the paper outlines such a technique.

3. Analytical background

Consider a V-shaped notch with an opening angle 2β, as shown in Figure 1. In Ref. [16] it was proven that, provided the material is homogeneous, isotropic, and has linear thermo-elastic behaviour, the equations representing the stress field near the V-notch are independent of the thermal constants and match the exact solution obtained by Williams [17].
Accordingly, the resulting linear-elastic plane-stress and plane-strain stress field near the notch tip can be described by the following equation:

$$\sigma_{ij}(r,\theta) = \frac{K_I^{th}}{r^{1-\lambda_I}} g_{ij}(\theta) \quad (i,j = r,\theta) \tag{1}$$

where $g_{ij}(\theta)$ are the angular functions, λ_I is the Williams' eigenvalue, coming from the solution of Eq. (2):

$$\lambda \sin(2\gamma) + \sin(2\lambda\gamma) = 0 \quad \text{with } \gamma = \pi - \beta \tag{2}$$

and K^{th}_I is the NSIF due to a thermal symmetric load (opening mode I) which can be determined according to the definition proposed by Gross and Mendelson [24]:

$$K_I^{th} = \sqrt{2p}\lim_{r\to 0} r^{1-l_1}\sigma_{qq}(r,\theta=0) \tag{3}$$

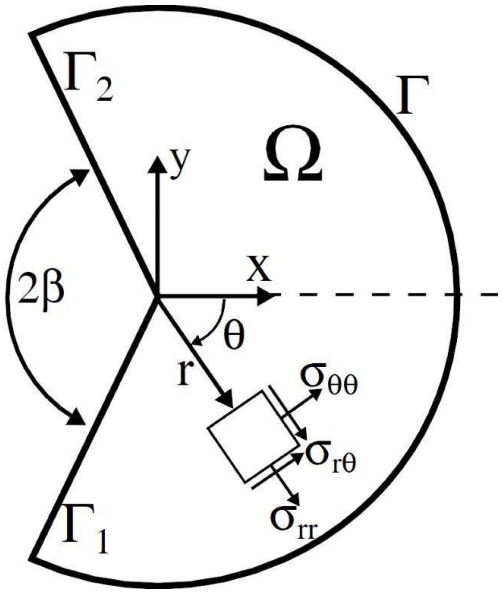

Fig. 1 - Domain Ω for the sharp V-notch problem

As evident from Eq. (2), λ_1 explicitly depends only on the V-notch angle (2β) and varies from 0.5 and 1. The eigenvalue is 0.5 in the crack case (2β=0), and increases to 0.674 and 0.757 when the angle is 135 and 150 degrees, respectively. The corresponding degrees of singularity of the stress field then become 0.5, 0.326 and 0.243. If the stress field is known, it is also possible to evaluate the strain energy density averaged over a semicircular sector (control volume) surrounding the singularity point:

$$\bar{W} = \frac{e_1}{E}\left[\frac{K_I^{th}}{R_C^{1-l_1}}\right]^2 \tag{4}$$

where the control radius (R_C) is a material characteristic parameter [15], whereas e_I depends on the V-notch opening angle (2β), Poisson's ratio (ν), and the failure hypothesis employed. In the case of the Beltrami failure criterion, in plane strain conditions, ν = 0.34 (aluminium alloy AA 6063) and 2β = 135°, e_I is equal to 0.111.

4. Welding numerical simulation

4.1 Thermo-metallurgical and mechanical simulation

The welding of 6063 Al-alloy sheets described in Ref. [8] was simulated by means of Sysweld® numerical code. Plates were welded in the double V configuration using the GMAW technique and the ER4043 alloy as filler metal. The specimen geometry is shown in Fig. 2. By taking advantage of several analyses of aluminium welded joints [15] and the geometry of the numerical model provided in Ref. [8], the weld toe was modelled as a sharp V-notch with an opening angle equal to 135°. Thermo-metallurgical and mechanical properties of the filler and base metal were taken from Sysweld database.

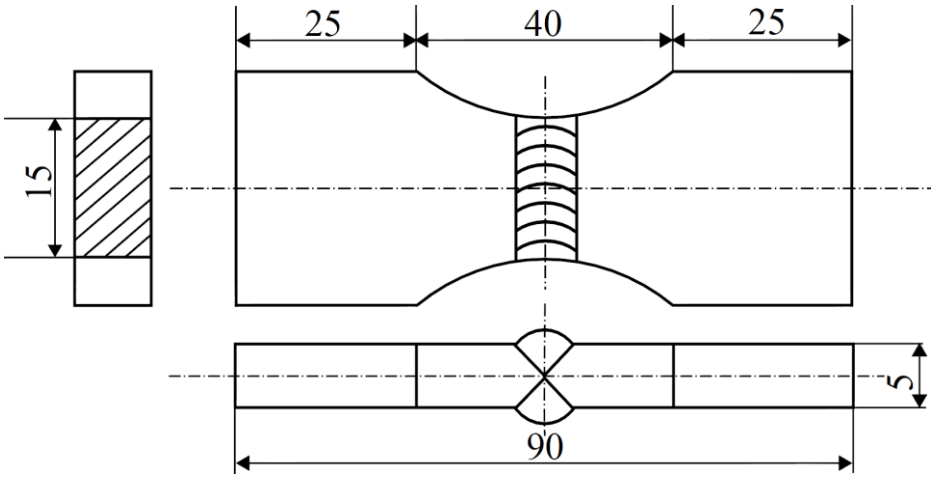

Fig. 2 – Geometry of the specimen (mm)

In order to simulate the softening effect induced by welding in the heat affected zone (HAZ), dissolution of β”(Mg_2Si) precipitates was taken into account by means of the following reversion model [25]:

$$f = \left(\frac{t}{t_r^*}\right) \exp\left[\frac{Q_s}{R^g} + \frac{nQ_d}{R^g}\left(\frac{1}{T_r} + \frac{1}{T}\right)\right] \tag{5}$$

In Eq. (5) f is the dissolution fraction of precipitates, t is the time, T is the temperature (K), R^g is the constant of perfect gas, t_r^* is the time necessary for the total dissolution of precipitates at a given temperature T_r, Q_s is the enthalpy of metastable solvus, Q_d is the energy for activation of diffusion process of one of alloy elements (the less mobile) and, finally, n is a parameter which depends on f. The yield stress in the HAZ has been calculated by using the following linear mixture law:

$$s_y = f \times s_y^{SHT} + (1 - f) \times s_y^{T6} \quad (6)$$

where σ_y^{SHT} and σ_y^{T6} are the yield stresses of the material at solution heat treated (SHT) and T6 condition, respectively. Radiative (*Stephan-Boltzman Law*) and convective heat losses were considered on the free edges of the plate. For convective heat losses, a convective heat transfer coefficient equal to $25 \cdot 10^{-3}$ W/mm was used. The arc-welding torch was modelled by means of Goldak's source [26], according to the following equation:

$$q_g(x,y,t) = \frac{6\sqrt{3}\, f_{1,2}\, Q}{\pi\sqrt{\pi}\, a\, b\, c_{1,2}} e^{-\frac{3x^2}{a^2}} e^{-\frac{3y^2}{b^2}} e^{-\frac{3[v(t-\tau)]^2}{c_{1,2}}} \quad (7)$$

Eq. (7) describes the power density distribution arising by the intersection of the heat source with the section representing the 2D model [16]. All parameters are summarised in Table 1.

Q*	Power input [W]	2860
η	Efficiency	0.64
Q	Absorbed power [W], with Q=ηQ*	1830
a	Molten pool dimensions [mm]	4
b		1.5
c_1		2.3
c_2		7.9
f_1	Constants for the energy distribution of the heat flux	0.6
f_2		1.4
v	Welding speed [mms^{-1}]	11
τ	Total time spent by the welding source to be over the transverse cross section of the plate [s]	35

Table 1 - Goldak's source parameters.

The source parameters values were calculated by matching the experimental microhardness profile across the weld bead with that numerically calculated by means of the following linear mixture law (reverse analysis):

$$HV = f \times HV^{SHT} + (1 - f) \times HV^{T6} \quad (8)$$

where HV^{T6} and HV^{SHT} are the Vickers hardness of the material in the T6 (85 kg/mm^2) and solution heat treated (SHT) (50 kg/mm^2) condition, respectively. Finally, fusion zones were modelled by element birth method.

Since the analysis of the singular stress state at the weld toe requires very refined meshes, the problem size was reduced by using a 2D FE model under generalized plane-strain conditions [27-29] (Fig. 3). Because of the double symmetry of the geometry, it was only necessary to model one half of the joint using some 5500 parabolic isoparametric elements. At the notch tip, the minimum size of the elements was approximately 5×10^{-4} mm. Finally, an uncoupled, thermo-mechanical analysis was carried out by using SYSWELD® code.

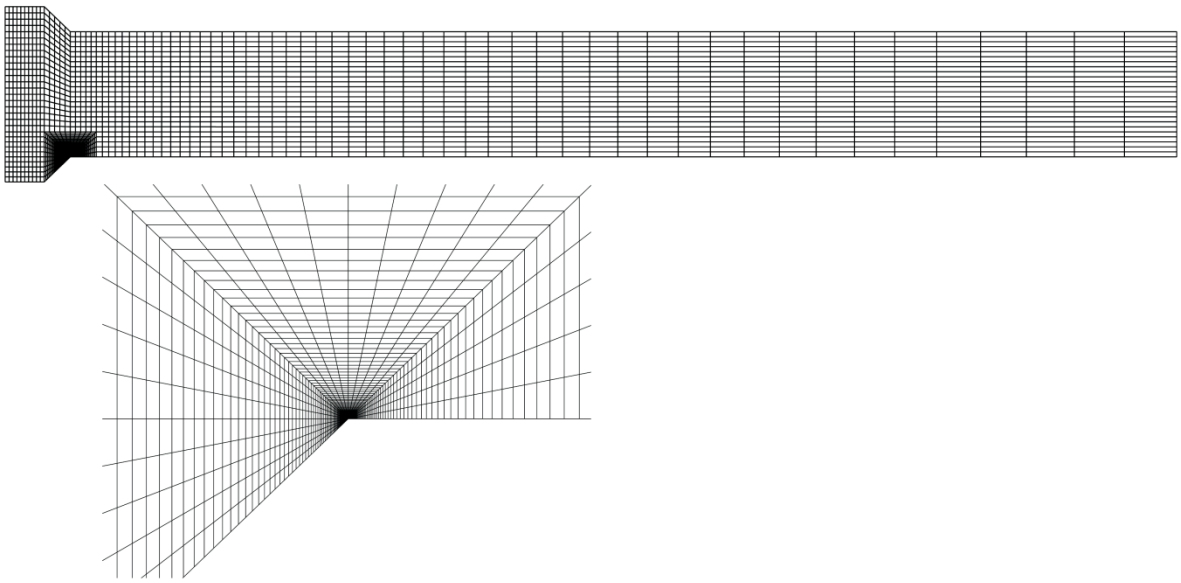

Fig. 3 – FE model of the welded joint

4.2 Fatigue loading simulation

Four-point bending fatigue tests were simulated by applying a ten cycles of fatigue load as shown in Fig. 4. At room temperature the material was assumed to behave according to the modified Ramberg–Osgood law with kinematic strain hardening (n = 5) (yield strength equal to 190 MPa). The fatigue load was characterized by a stress ratio $R^L = 0$ and a sawtooth waveform. The nominal stress amplitude ($\Delta\sigma_n$) was varied at each analysis from 25 to 120 MPa in order to study the effect of the increasing plasticization near the notch tip on the initial residual stress distribution.

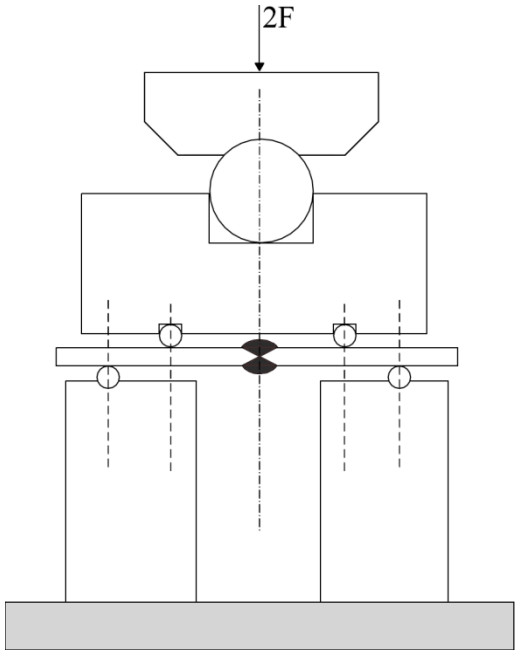

Fig. 4 – Configuration of the fatigue tests [8]

5. Results and discussion

Fig. 5 shows the calculated asymptotic distribution of in-plane residual stresses near the weld toe of the bottom side of the joint together with the out of plane and von Mises equivalent stress. Since negative in-plane residual stresses were obtained, their absolute value is plotted in the log-log diagram. A good correlation is found between the numerical and analytical elastic solution by Williams [17]. Due to the mixed mode loading, the analytical solution contains also the Mode II component that is not singular for the analysed V-notch opening angle and the first term (Mode I) dominates up to about 0.15 mm from the notch tip. In particular, the NSIF of the asymptotic residual stress field (K_I^{res}) was found equal to -8.3 MPa $mm^{0.3264}$. An uncoupled behaviour is observed between the in-plane and out-of-plane stress components with the out-of-plane stress working in the elastic-plastic field. During loading, it is expected that the redistribution takes place if the von Mises stress exceeds the cyclic yield strength.

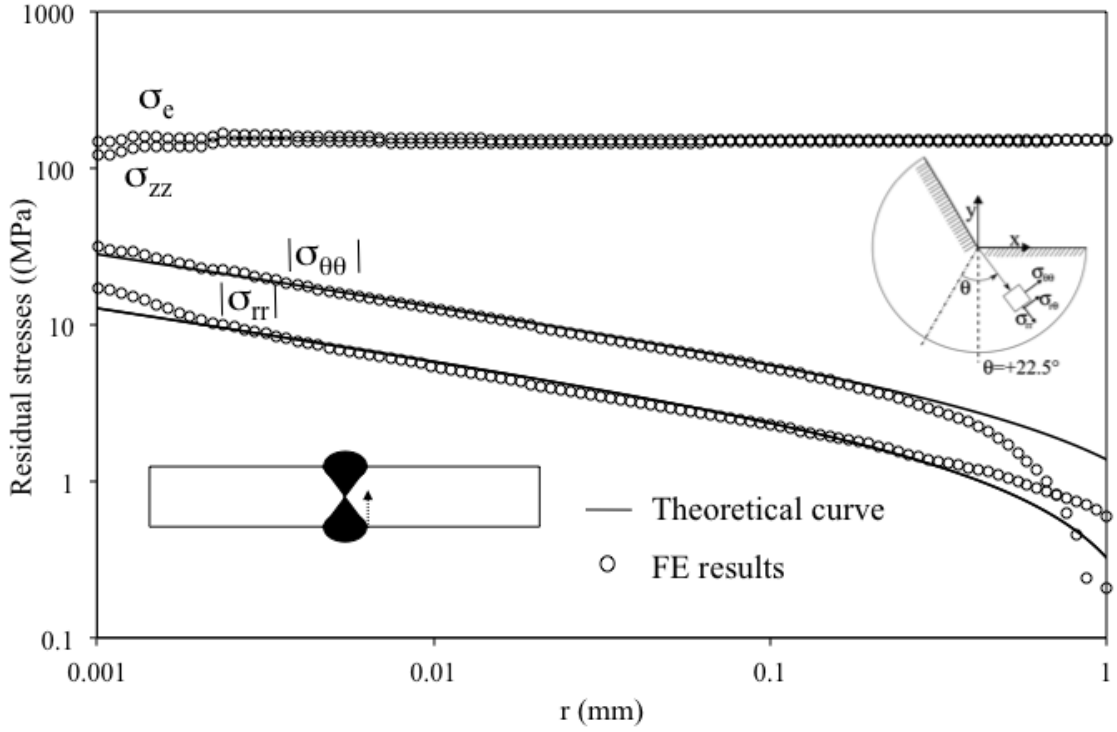

Fig. 5 - Residual stress distribution at θ =22.5° (transverse residual stresses) (K_I^{res}=-8.3 MPa $mm^{0.3264}$, K_{II}^{res}= 5 MPa $mm^{-0.3021}$).

It was observed that the residual stresses behaviour under cyclic loading depends on load amplitude. Fig. 6 illustrates the variation of asymptotic transverse residual stresses in the as-welded joint under different cyclic loading cases. Any redistribution of the residual stress occurs during loading ($\Delta\sigma_n$ = 25 MPa) in the first cycle and the distribution remains stable during the successive load cycles. In the low yield strength aluminium alloy analysed, residual stress redistribution takes place at low load amplitudes. For this reason, reduced fatigue strength sensitivity on initial residual stress is expected even in the high cycle fatigue conditions compared to high strength alloys. Regardless of high or low cycle fatigue conditions, the initial redistribution can be described by using the von Mises failure criterion.

As a matter of fact, the greater the stress amplitude ($\Delta\sigma_n$), the greater the distance (R_p) from the weld toe where the von Mises maximum stress (σ_e) equals the yield stress (Fig. 6). Finally, the greater the R_p value, the greater the degree of residual stress redistribution.

Fig. 7 shows the residual stress distribution after ten cycles in stress-relieved welded joint. It is observed that where plasticity occurs ($0 < r < R_p$) the residual stress distribution of stress-relieved welded joins approximates that of the as-welded joints and matches the elastic-plastic solution [16,18].

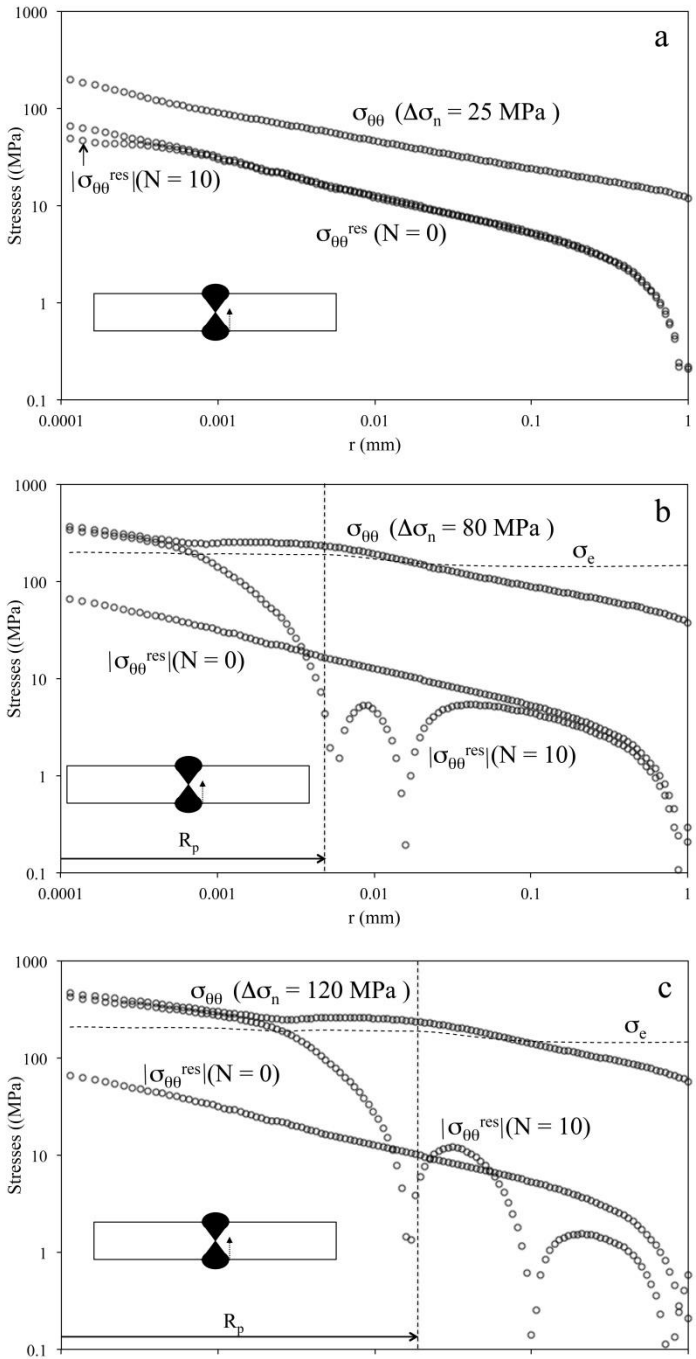

Fig. 6 – Residual stress redistribution of the as-welded joint after ten cycles and maximum transverse stress field (θθ component) at different values of the remotely applied stress amplitude ($\Delta\sigma_n$); $\Delta\sigma_n$ = 25 MPa (a), $\Delta\sigma_n$ = 80 MPa (b), $\Delta\sigma_n$ = 120 MPa (c).

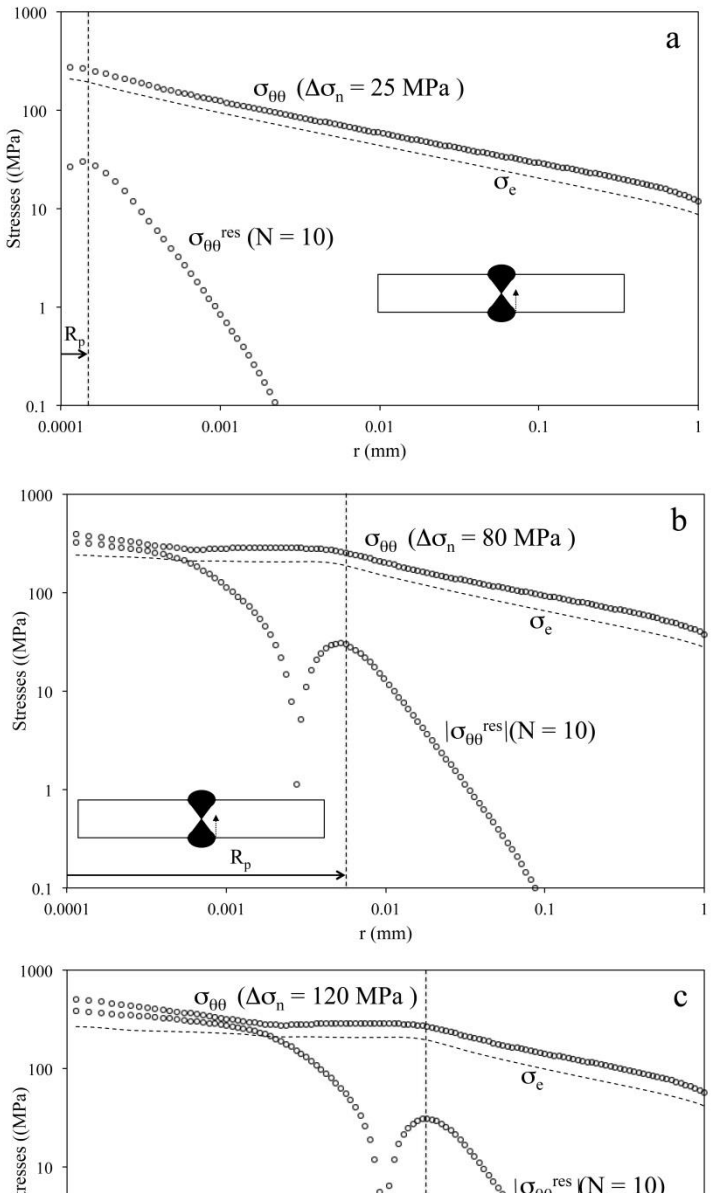

Fig. 7 – Illustration of the residual stress redistribution of the stress-relief welded joint after ten cycles of loading and of maximum transverse stress field (θθ component) at different values of the remotely applied stress amplitude ($\Delta\sigma_n$); $\Delta\sigma_n$ = 25 MPa (a), $\Delta\sigma_n$ = 80 MPa (b), $\Delta\sigma_n$ = 120 MPa (c).

By comparing the maximum transverse stress field of as-welded and stress-relieved joints (Fig. 8), it can be observed that the greatest difference is obtained when the two stress distributions are elastic. On the other hand, when residual stress redistribution occurs, the two stress fields tend to overlap, showing a reduction of fatigue strength sensitivity on initial residual stresses.

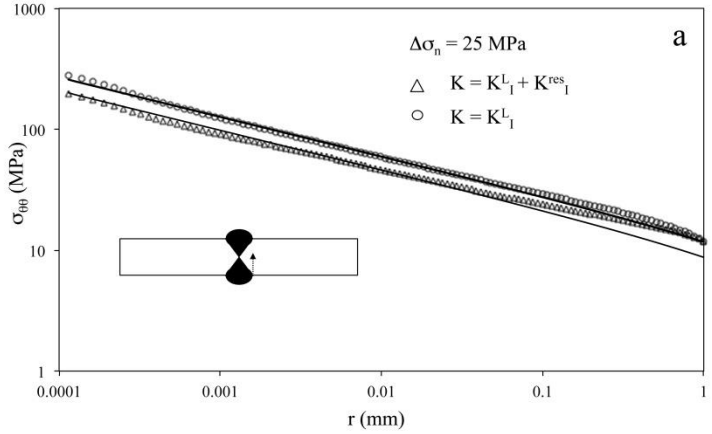

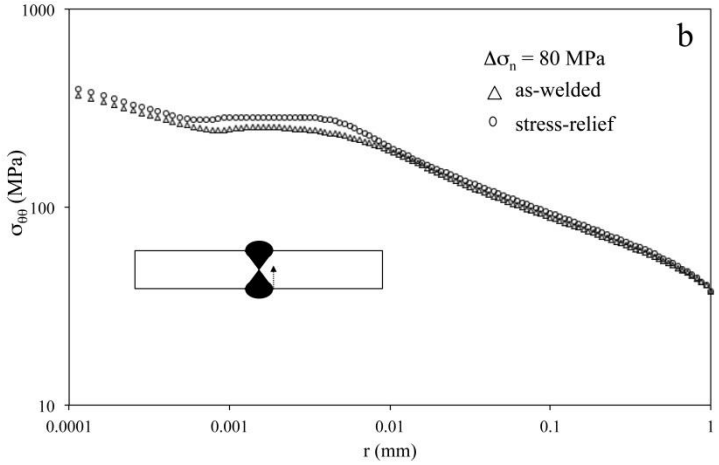

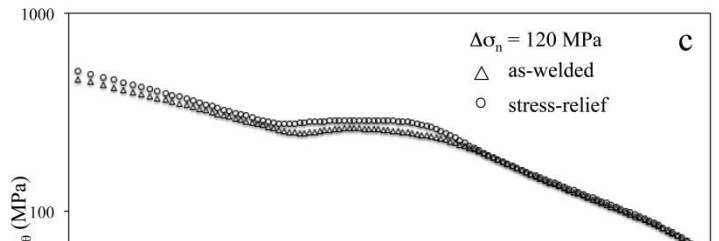

Fig. 8 – Maximum transverse stress field (θθ component) of stress-relief and as-welded joint after ten cycles at different values of the remotely applied stress amplitude ($\Delta\sigma_n$); $\Delta\sigma_n$ = 25 MPa (a), $\Delta\sigma_n$ = 80 MPa (b), $\Delta\sigma_n$ = 120 MPa (c).

Once the NSIFs associated to the residual stress fields are known, the evaluation of their influence on the fatigue strength of the component can be tackled by using the SED approach. Indeed, the following equations hold valid [23]:

$$\left.\begin{array}{l} \Delta K = K_{I_{max}}^{L} - K_{I_{min}}^{L} \\ R = \dfrac{K_{I_{min}}^{L} + K_{I}^{res}}{K_{I_{max}}^{L} + K_{I}^{res}} \\ R = \dfrac{K_{I_{min}}^{L}}{K_{I_{max}}^{L}} \end{array}\right\} \quad K_{I_{min}}^{L} + K_{I}^{res} > 0 \qquad \left.\begin{array}{l} \Delta K = K_{I_{min}}^{L} + K_{I}^{res} \\ R = 0 \end{array}\right\} \quad K_{I_{min}}^{L} + K_{I}^{res} \le 0 \tag{9}$$

where K_I^L is the NSIF of the stress field induced by the applied load, K_I^{res} is the NSIF associated to the residual stress field, R^L is the conventional load ratio, whereas R is the local load ratio which accounts for welding residual stresses.

Invoking the relations linking the NSIFs to the SED value, $\overline{W}$, the following analytical expressions can be obtained [23]:

$$\Delta s_n = \frac{R_C^{1-l_I}\left[\dfrac{E}{e_I}\left(\dfrac{C}{N}\right)^{1/z}\right]^{1/2}}{k_I h^{1-l_I}} - \frac{K_I^{res}}{k_I h^{1-l_I}} \tag{10}$$

for R=0 and,

$$\sigma_{max}^{L} = \frac{\left(\left(K_I^{res}\right)^2 + \frac{(1+R^L)}{(1-R^L)}\frac{E}{e_I}R_C^{2(1-\lambda_1)}\left(\frac{C}{N}\right)^{1/z}\right)^{1/2}}{k_I h^{1-\lambda_1}(1+R^L)} - \frac{K_I^{res}}{k_I h^{1-\lambda_1}(1+R^L)} \quad (11)$$

for R>0. In Eqs. (10,11) C is a constant and z is the slope of the fatigue curve expressed in terms of local strain energy density experimentally calculated ($z = \mathrm{Log}(N_{D_1}/N_{D_2})/\mathrm{Log}(\Delta\bar{W}_{D_2}/\Delta\bar{W}_{D_1})$, subscripts D_1 and D_2 indicate two points of the curve $\Delta\bar{W}(N)$); k_I is a non-dimensional coefficient, analogous to the shape functions of cracked components calculated by using the following equation:

$$K_I^m = k_I \sigma_n h^{1-\lambda_1} \quad (12)$$

where σ_n is the remotely applied stress, and h is a geometrical parameter of the plate, defined by Lazzarin and Tovo [13]. By using the plate thickness (5 mm) as the reference dimension (h), k_I is easily found to be equal to 0.976. Fatigue data of stress-relieved samples published in Ref. [8] are used to calculate the fatigue curve expressed in terms of local strain energy density by means of Eq. (10) with K_I^{res} equal to 0 MPa $mm^{0.3264}$.
Equations (10) and (11) are applied in the high-cycle fatigue regime ($N > 2*10^6$), where the redistribution of pre-existing residual stresses are negligible. In the low-cycle fatigue regime ($N < 10^5$ cycles) the fatigue strength of as-welded and stress-relieved joints should be the same because of the residual stress redistribution induced by plastic effects. Under the condition $K_{Imin}^L + K_I^{res} < 0$, Fig. 9 shows an estimation of the fatigue resistance of the stress-relieved and as-welded component predicted by means of the proposed model, Eq. (10).

It is useful to note that cracks were always observed to nucleate at the weld root [8] where the local strain energy density has been calculated. Furthermore, due to the negative value of the residual NSIF, an improvement of fatigue strength of as-welded joints is observed experimentally and predicted by the model compared to the fatigue strength of the stress-relief specimens. It is also worth mentioning that in real welded joints, coupled effects arise among modes I, II and III, which can be captured only using 3D models [30] and this aspect will be investigated in a future work.

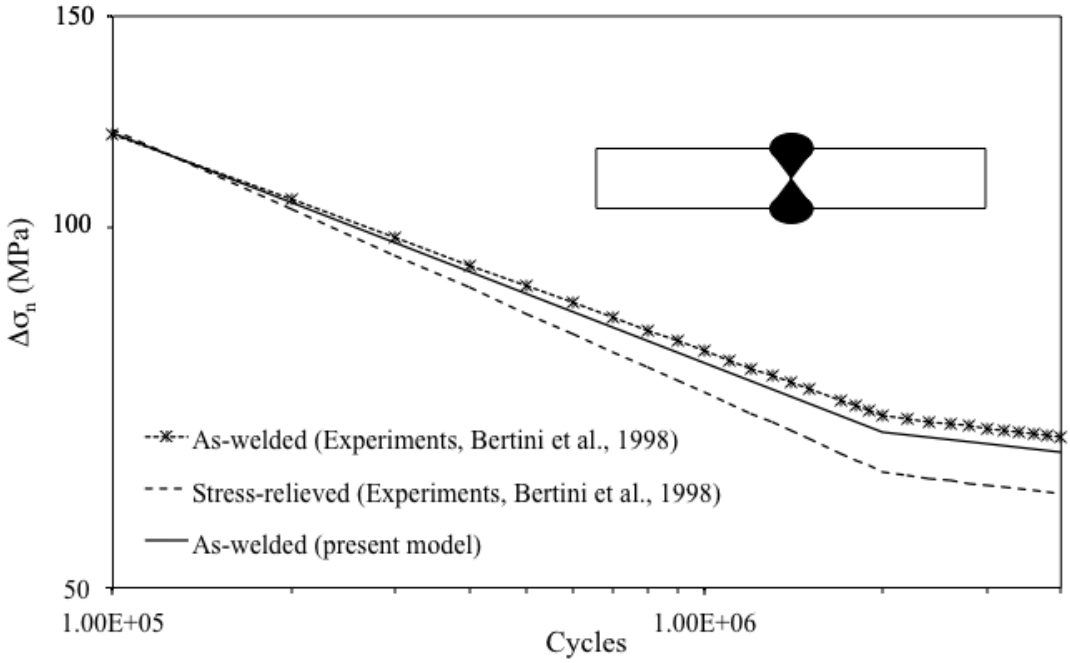

Fig. 9 - Residual stress influence on the fatigue strength of the butt welded joint predicted by the present model (R_c = 0.12 mm [15]).

5. Conclusions

The present numerical residual stress analysis of Al-6063 butt-welded joints has shown that its distribution near the weld toe follows the Williams elastic solution only for the in-plane components. Regardless the value of the applied fatigue load, redistribution of residual stress takes place during the very first load cycles. In high cycle fatigue loading, except for a small redistribution very close to the notch tip, little redistribution of residual stress was predicted. This implies that, in the range of high cycle fatigue, the fatigue strength sensitivity to the initial residual stresses is expected to be high. On the contrary, during low cycle fatigue, redistribution takes place during the very first load cycles. The major portion of the redistribution occurs in the zone where the von Mises stress exceeds the yield strength. At high fatigue loads the in-plane stress field of stress-relieved and as-welded joints almost overlap making the fatigue strength insensitive to the initial residual stress distribution.

In the high cycle regime where the redistribution of residual stresses induced by plastic effects is negligible (the *small scale yielding* hypothesis) a method based on the strain energy density approach was used to quantify the effects of residual stresses on the fatigue strength of welded joints. On the other hand, the fatigue strength of as-welded joints in the low-cycle regime was set equal to that of stress-relieved specimens. Because of the negative value of the residual NSIF, an improvement in fatigue strength is predicted by the model in the high cycle regime for the as-welded joints compared to those that were stress-relieved. The experimental and predicted results were found to be in good agreement.

References

[1] Wilson M and Wilder A.B. (1939). Fatigue tests of butt welds in structural steel plates. Univ. Illinois Engng Exp. Station Bull, 310.

[2] Ros M. (1950) Experiments for the determination of the influence of residual stresses on the fatigue strength of structures. *Weld. Res*. BWRA, 4, 83r–93r.

[3] Soete W. and Crombrugge V. (1950). A study of the fatigue strength of welded joints. *Rev. Soudure. Las-tijdscrift*, 6, 72–82.

[4] Soete W. and Crombrugge V. (1952). A study of the fatigue strength of welded joints. *Welding J*., 2, 100s–103s.

[5] Kudryavtsev I.V., The influence of internal stresses on the fatigue endurance of steel. Int. Conf. on Fatigue. I. Mech. E. 1956 p. 317

[6] Trufyakov V.I. (1956). The role of residual stresses in reducing the endurance of welded joints. *Automatecheskaya Svarka*, 5, 90–103.

[7] Trufyakov V.I. (1958). Welded joints and residual stresses. *Br. Weld. J.*, 5, 491–498.

[8] Bertini L., Fontanari V. and Straffellini G. (1998). Influence of post weld treatments on fatigue behaviour of Al-alloy welded joints. *Int. J. Fatigue*, 20, 749–755.

[9] Radaj D. Ermudungsfestigkeit, Fatigue Strength, Springer Verlag, 1995

[10] Haibach E., Betriebsfestigkeit, Fatigue Strength in Service, 2.Aufl., Springer Verlag, 2002

[11] EN 1993-1-9 (Eurocode 3): Design of Steel Structures, Part 1.9: Fatigue Strength of Steel Structures, CEN, Brussels, Belgium, 2005

[12] Gurney T.R., Fatigue of welded structures, Cambridge University Press, 1968

[13] Lazzarin P., Tovo R. (1998). A Notch Intensity Approach to the Stress Analysis of Welds. *Fatigue Fract. Engng Mater. Struct.*, 21,1089-1104.

[14] Lazzarin P. and Zambardi R. (2001). A finite-volume-energy based approach to predict the static and fatigue behavior of components with sharp V-shaped notches. *Int. J. Fract.*, 112, 275–298

[15] Livieri P. and Lazzarin P. (2005). Fatigue strength of steel and aluminium welded joints based on generalised stress intensity factors and local strain energy values. *Int. J. Fract.*, 133, 247–76

[16] Ferro P., Berto F., and Lazzarin P. (2006). Generalized stress intensity factors due to steady and transient thermal loads with applications to welded joints. *Fatigue Fract. Eng. Mater. Struct.*, 29, 440–453

[17] Williams M.L. (1952). Stress singularities resulting from various boundary conditions in angular corners of plates in extension. *J. Appl. Mech.*, 19, 526-528.

[18] Lazzarin P., Zambardi R., Livieri P. (2001). Plastic Notch Stress Intensity Factors for Large V-Shaped Notches under Mixed Load Conditions. *Int. J. Fracture*, 107, 361-377

[19] Ferro P., Bonollo F. and Tiziani A. (2010). Methodologies and experimental validations of welding process numerical simulation. *Int. J. Comput. Mater. Sci. Surf. Eng*., 3, 114–132.

[20] Ferro P., Porzner H., Tiziani A. and Bonollo F. (2006). The influence of phase transformation on residual stresses induced by the welding process—3D and 2D numerical models. *Modell. Simul. Mater. Sci. Eng*., 14, 117–136.

[21] Ferro P. and Petrone N. (2009). Asymptotic thermal and residual stress distribution due to transient thermal loads. *Fatigue Fract. Eng. Mater. Struct*., 32, 936–948

[22] Ferro P. (2012). Influence of phase transformations on the asymptotic residual stress distribution arising near a sharp V- notch tip. *Modell. Simul. Mater. Sci. Eng*., 20, DOI: 10.1088/ 0965-0393/20/8/085003

[23] Ferro P. (2014). The local strain energy density approach applied to pre-stressed

components subjected to cyclic load. *Fatigue Fract. Eng. Mater. Struct*., 37, 1268–1280

[A] British Standards Institution (2013). Guide to methods for assessing the acceptability of flaws in metallic structures, BS 7910:2013.

[B] Zhang, Yan-Hui, Smith, S., Wei, Liwu and Johnston, C. (2012). Residual stress measurements and modelling, Research Report RR938, Health and Safety Executive, London.

[C] James, M. N. (2011). Residual stress influences on structural reliability, *Engineering Failure Analysis*, 18 1909-1920.

[D] Smith, D. J., Farrahi, G. H., Zhu, W. X. and McMahon, C. A. (2001). Obtaining multiaxial residual stress distributions from limited measurements. *Materials science and Engineering*, A303 281-291.

[E] Deng, D. and Kiyoshima, S. (2010). Numerical simulation of residual stresses induced by laser beam welding in a SUS316 stainless steel pipe with considering initial residual stress influences. *Nuclear Engineering and Design*, 240 688-696.

[F] Acevedo, C. and Nussbaumer, A. (2012). Effect of tensile residual stresses on fatigue crack growth and S–N curves in tubular joints loaded in compression. *International Journal of Fatigue*, 36 171-180.

[G] Bussu, G. and Irving, P.E. (2003). The role of residual stress and heat affected zone properties on fatigue crack propagation in friction stir welded 2024-T351 aluminium joints. *International Journal of Fatigue*, 25 77-88.

[H] Bertini, L. (1991). Influence of seawater and residual stresses on fatigue crack growth in C-Mn steel weld joints. *Theoretical and Applied Fracture Mechanics*, 16 135-144.

[I] Cho, J. and Lee, C-H. (2015). FE analysis of residual stress relaxation in a girth-welded duplex stainless steel pipe under cyclic loading. *International Journal of Fatigue*, in press. doi/10.1016/j.ijfatigue.2015.09.001

[J] Lee, C-H., Chang, K-H. And Van Do, V. N. (2015). Finite element modelling of residual stress relaxation in steel butt welds under cyclic loading. *Engineering Structures*, 103 63-71.

[K] Li, L., Wan, Z., Wang, Z. and Ji, C. (2009). Residual stress relaxation in typical weld joints and its effect on fatigue and crack growth. *Acta Metall. Sin. (Engl. Lett.)* 22 3 202-210.

[L] Hao, H., Ye, D., Chen, Y. Mi, F. And Liu, J. (2015). A study on the mean stress relaxation behavior of 2124-T851 aluminum alloy during low-cycle fatigue at different strain ratios. *Materials and Design*, 67 272-279.

[M] Hatamleh, O., Rivero, I. V. and Swain, S. E (2009). An investigation of the residual stress characterization and relaxation in peened friction stir welded aluminum–lithium alloy joints. *Materials and Design*, 30 3367-3373.

[N] Esderts, A., Willen, J. and Kassner, M. (2012). Fatigue strength analysis of welded joints in closed steel sections in rail vehicles. *International Journal of Fatigue*, 34 112-121.

[O] James, M. N., Hattingh, D. G., Hughes, D. J., Wei, LiWu, Patterson, E.A. and Quinta da Fonseca, J. (2004), Synchrotron diffraction investigation of the distribution and influence of residual stresses in fatigue. *Fatigue Fract. Engng Mater. Struct.* 27, 609–622.

[P] Newby, M., James, M. N. and Hattingh, D. G. (2014). Finite element modelling of residual stresses in shot-peened steam turbine blades. *Fatigue Fract. Engng Mater. Struct.* 37 707-716.

[Q] Asquith, D. T., Hughes, D. J., Hattingh, D. G., James, M. N. and Yates, J. R. (2007). Re-orientation of residual strains under cyclic loading, Fatigue 2007, Eds. M.R.

Bache, P.A. Blackmore, E.R. Cawte, P. Roberts and J.R. Yates, Proceedings of the 6th International Conference on Durability and Fatigue, 26-28 March 2007, Cambridge, UK.

[24] Gross R and Mendelson A (1972). Plane elastoplastic analysis of V-notched plates. *Int. J. Fract. Mech,* 8, 267-76

[25] Grong Ø. Metallurgical Modelling of Welding. Second Edition. Materials Modelling Series. The Institute of Materials, 1997 University Press, Cambridge, UK.

[26] Goldak, J., Chakravarti, A. and Bibby, M. (1984) A new finite element model for welding heat sources. *Metallur. Trans. B* **15b**, 299–305.

[27] Mok, D.H.B.and Pick, R.J.(1991). Finite element study of residual stresses in a plate T-joint fatigue specimen, *Int. J. Fatigue* **13**, 281-291.

[28] Sarkani, S., Tritchkov, V. and Michaelov, G. (2000). An efficient approach for computing residual stresses in welded joints, *Finite Elements Anal. Design* **35**, 247-268.

[29] Teng, T.L., Fung, C.P., Chang, P.H. and Yang, W.C. (2001). Analysis of residual stresses and distortions in T-joint fillet welds, *Int. J. Pressure Vessels Piping* **78**, 523-538.

[30] Lazzarin P, Zappalorto M and Berto F (2015). Three dimensional stress fields due to notches in plates under linear elastic and elastic–plastic conditions. *Fatigue Fract. Eng. Mater. Struct*. DOI: 10.1111/ffe.12138